Route of a Multipartite Nanovirus across the Body of Its Aphid Vector

Jérémy Di Mattia, Marie-Stéphanie Vernerey, Michel Yvon, Elodie Pirolles, Mathilde Villegas, Yahya Gaafar, Heiko Ziebell, Yannis Michalakis, Jean-Louis Zeddam, Stéphane Blanc

Title: Route of a multipartite (nano)virus across the body of its aphid vector

Authors:

Jérémy Di Mattia[1], Marie-Stéphanie Vernerey[1], Michel Yvon[1], Elodie Pirolles[1], Mathilde Villegas[1], Yahya Gaafar[2], Heiko Ziebell[2], Yannis Michalakis[3], Jean-Louis Zeddam[1,4,#], Stéphane Blanc[1,*,#]

Affiliation:

[1] UMR BGPI, Inrae, Cirad, Montpellier SupAgro, Univ. Montpellier, Montpellier, France

[2] Julius Kühn-Institut, Messeweg 11/12, 38104 Braunschweig, Germany

[3] MIVEGEC, Cnrs, Ird, Univ Montpellier, Montpellier, France

[4] UMR IPME, Ird, Cirad, Univ. Montpellier, Montpellier, France

[#] Both authors equally contributed to the work

* Send correspondence to: stephane.blanc@inra.fr.

Abstract:

Vector transmission plays a primary role in the life cycle of viruses and insects are the most common vectors. An important mode of vector transmission, reported only for plant viruses, is the circulative non-propagative transmission where the virus cycles within the body of its insect vector, from gut to salivary glands and saliva, without replicating. This mode of transmission has been extensively studied in the viral families *Luteoviridae* and *Geminiviridae* and is also reported for *Nanoviridae*. The biology of viruses within these three families is different and whether they have evolved similar molecular/cellular virus-vector interactions is unclear. In particular, nanoviruses have a multipartite genome organization and how the distinct genome segments encapsidated individually transit through the insect body is unknown. Here, using a combination of fluorescent in situ hybridization and immuno-fluorescence, we monitor distinct proteins and genome segments of the nanovirus *Faba bean necrotic stunt virus* (FBNSV) during transcytosis through the gut and salivary gland cells of its aphid vector *Acyrthosiphon pisum*. FBNSV specifically transits through cells of the anterior midgut and principal salivary gland cells, a route similar to geminiviruses but distinct from luteoviruses. Our results further demonstrate that a large number of virus particles enter every single susceptible cells, so that distinct genome segments always remain together. Finally, contrasting with the two other viral families mentioned here, we confirm that the success of nanovirus-vector interaction depends on a non-structural helper component, the viral protein NSP, which is shown to be mandatory for viral accumulation within gut cells.

47 **Importance**

48 An intriguing mode of vector-transmission described only for plant viruses is the circulative non-
49 propagative transmission, where the virus passes through the gut and salivary glands of the insect vector
50 without replicating. Three plant virus families are transmitted this way, but details of the
51 molecular/cellular mechanisms of the virus-vector interaction are missing. This is striking for nanoviruses
52 that are believed to interact with aphid vectors in ways similar to luteoviruses or geminiviruses but for
53 which empirical evidence is scarce. We here confirm that nanoviruses follow a within-vector route
54 similar to gemini- but distinct from luteoviruses. We show that they produce a non-structural protein
55 mandatory for viral entry into gut cells, a unique phenomenon for this mode of transmission. Finally,
56 nanoviruses being multipartite viruses, we demonstrate that a large amount of viral particles penetrate
57 susceptible cells of the vector, allowing distinct genome segments to remain together.

58

Introduction

Among hundreds of plant virus species recognized by the International Committee on Taxonomy of Viruses (ICTV), nearly 80% are transmitted from plant-to-plant by vector (1). Vectors can be very diverse plant-feeding organisms or parasites (insects, mites, nematodes and protists) but Hemipteran insects (2) and particularly aphids and whiteflies are by far the most important (1, 3). There are distinct categories of virus-vector interactions, named circulative or non-circulative depending on whether the virus penetrates and circulates within the body of its vector or more simply attaches externally to the cuticle of its mouthparts (4). In the circulative transmission, the virus often replicates in the vector, as is the case for all arboviruses infecting vertebrates and for a few plant viruses in the families *Tymo-*, *Rhabdo-*, and *Reoviridae* or in the order *Bunyavirales*. An intriguing variation of the circulative transmission, qualified as non-propagative, has solely been reported in plant viruses (5). In this case, the virus circulates through the gut to the salivary gland cells of its insect vector, but does not replicate during this process (6).

Circulative non-propagative transmission has been reported for three economically important families of plant viruses: *Luteo-*, *Gemini-* and *Nanoviridae*. In each case, the molecular/cellular interaction between virus and vector is not fully elucidated, and whether viruses in these three families follow similar pathways in their respective vectors is unclear. A series of pioneering electron microscopy studies have revealed the accumulation of virus particles of distinct luteovirus species in clathrin-coated vesicles of midgut or hindgut (7-9) cells of their aphid vectors. These vesicles seemingly follow the early endosomal pathway prior to the appearance of non-coated tubular vesicles within which the virions are believed to reach the basal membrane and exit gut cells into the hemolymph (10). The transcytosis process has been shown to be similar when luteovirids cross the accessory salivary gland cellular barrier (9). For geminiviruses, and particularly the best studied genus *Begomovirus*, a number of reports used immunolabeling of the coat protein to demonstrate that virus particles also use a clathrin-assisted endocytosis process, following the early endosomal pathway (11). The specific receptors at the level of the gut lumen are poorly known in circulative non-propagative transmission. Only two receptor-candidates, the amino-peptidase N and the Ephrin receptor protein, have been identified for luteoviruses (12-14), whereas no such candidates could be identified for geminiviruses. In both families, the process by which virus particles internalized in gut/salivary gland cells successfully exit the cells and escape the endosome recycling and lysosome pathway is not understood. It has been shown that the transit of the geminivirus *Tomato yellow leaf curl virus* (TYLCV) across its whitefly gut cells triggers

autophagy as an insect-defense mechanism (15). Such a process is not reported to date for luteoviruses. Despite important differences in their life history, the transmission mode and the virus-vector interaction for nanoviruses is mostly inferred from knowledge acquired from geminivirus species. Very scarce empirical information is available for nanoviruses and further investigation is needed to better comprehend the circulative non-propagative transmission, its commonalities and specificities among the three viral families.

The family *Nanoviridae* comprises two genera, *Babuvirus* and *Nanovirus.* Their genome is respectively composed of six and eight single-stranded circular DNA molecules of approx. 1 kb (**Figure 1**). Each genome segment encodes a single protein and is individually encapsidated in an icosahedral particle of 17 to 20 nm in diameter (16). All viruses of this family are transmitted by aphids (16), and one series of studies describes the route of the *Babuvirus* banana bunchy top virus (BBTV) in its vector *Pentalonia nigronervosa* (17-19). By immunofluorescence labeling of the coat protein, the BBTV particles were localized in the aphid anterior midgut (AMG) and principal salivary glands (PSG) (17), reminiscent of the situation reported for geminiviruses in whiteflies. However, considering the specificities of nanoviruses, two prominent questions have not been addressed and are exposed below.

One major aspect in the genome architecture of nanoviruses, contrasting with luteoviruses and (most) geminiviruses, is that they are multipartite and so the virus population within the plant is a mixture of 6 to 8 types of viral particles, each type containing a distinct genome segment (20). In order to ensure successful passage of the integral genome to a new host plant, it is assumed that at least one functional particle of each type must be transmitted (21). We recently published that the genome segments of faba bean necrotic stunt virus (FBNSV) do not all co-exist in individual plant cells and suggested that the infection proceeds within the host plant through functional complementation of the distinct genes across distinct cells (22). In this intriguing “pluri-cellular” way of life, the virus can colonize host cells with a low multiplicity of infection (MOI). In previous studies tracking the BBTV within its aphid vector (17-19), only the coat protein was monitored. The actual identity of genome segments was not documented and so whether nanoviruses invade individual vector cells with a small or large number of virus particles, allowing the distinct genome segments to “travel” all together or separately from gut to salivary glands is unknown.

Another important aspect of the transmission of nanoviruses has been uncovered two decades ago with the species *Faba bean necrotic yellows virus* (FBNYV). Through a series of sequential acquisition of highly and poorly transmissible virus isolates by aphid vectors, Franz and collaborators (23) concluded that, in

addition to the virus particles, a viral factor or helper component (HC) is required for virus transit through the vector. Recently, using agro-infectious clones where any segment can be omitted during agro-inoculation, it was demonstrated that the absence of segment N in the infected plant does not affect systemic infection but totally precludes aphid transmission (24). The authors provided strong evidence that the HC of nanoviruses is the segment N-encoded nuclear shuttle protein (NSP), whose mode of action now awaits investigation.

Here, we confirm the internalization of the distinct FBNSV genome segments within the AMG and the PSG of its aphid vector *Acyrthosiphon pisum*. We demonstrate that the virus particles penetrate the aphid cells in very high numbers allowing all genome segments to travel together in all colonized aphid cells, sharply contrasting with the situation recently described in host plants (22). We further show that the NSP protein is mandatory for viral accumulation into aphid gut cells. Finally, we observe that both proteins NSP and CP co-localize with the viral genome segments, suggesting that NSP-virus particle complexes are the viral form that cycles within the aphid body.

Results

FBNSV accumulates in the anterior midgut and primary salivary glands of *Acyrthosiphon pisum*.

We used Fluorescence In Situ Hybridization (FISH) to localize the FBNSV DNA in aphid gut and salivary gland cells. Total viral DNA was first targeted using a whole-genome probe directed against the coding sequences of all eight segments. In the aphid gut, a specific and strong fluorescent signal could be observed in most if not all cells of the AMG, while downstream posterior midgut and hindgut were rarely and never labeled, respectively (**Figure 2A-C**). At the intracellular level, most of the signal was observed as numerous cytoplasmic perinuclear fluorescent foci sometimes polarized on one side of the nucleus (**Figure 2B**). No viral DNA could be detected in nuclei, even in those cells with most intense signal.

In salivary glands, the viral DNA appeared exclusively accumulated in PSG and exhibited an intracellular pattern similar to that observed in AMG cells. Interestingly, the viral DNA appeared detectable only in specific cells of the PSG (**Figure 2D-F**). Based on Ponsen's descriptions (25) of the PSG anatomy (**Figure 2D**), we propose this specific area to correspond to type-4 cells (**Figure 2E**). Other cells of the PSG and accessory salivary glands were not detectably labeled indicating that they do not or poorly accumulate FBNSV DNA segments.

The eight FBNSV segments travel together in their insect vector.

FBNSV being a multipartite virus, and because its eight distinct genome segments have recently been shown to accumulate in distinct cells of the host plant (21), we investigated whether they travel together or separately during their journey across the body of the aphid vector. For this purpose, we prepared segment-specific probes with distinct fluorochromes, and used them by pairs. In sharp contrast to the situation earlier reported within host plants (**Figure 2H**), the two segments of the pair R/S appeared co-localized not only within AMG individual cells but also within each of the numerous fluorescent foci within these cells (**Figure 2G**). The overall fluorescent signal was always weaker when FISH was applied to salivary glands, indicating a general lower level of accumulation of FBNSV in this tissue. When labeling the segment pair U2/U4, however, the signal was sufficiently intense to similarly conclude that the two segments accumulate together in individual cells and most, if not in all, fluorescent foci within these cells (**Figure 2I**).

Such systematic co-localization of distinct genome segments was confirmed in the AMG with three additional segment pairs: M/U1, C/N and U2/U4 (**Figure 3A to C**). In the PSG, solely the additional pair M/U1 yielded a weak but detectable signal and, although barely visible, the intracellular fluorescent foci also appeared to contain both segments (**Figure 3D)**. The different intensity of the fluorescent signal in AMG and PSG is probably due to different viral accumulation in these respective organs. The average number of copies of all eight segments was $1.64 \times 10^{8\,(+/-\,1x10e7)}$ in the head, containing the PSG, and $8.34 \times 10^{9\,(+/-\,6x10e8)}$ in the rest of the body (see Materials and Methods). All together, these observations suggest that all FBNSV segments are internalized in gut and salivary gland cells of their insect vector and undergo transcytosis as groups of virus particles, large enough to contain one or more copies of each segment.

Viral DNA co-localizes with CP and NSP within aphid AMG cells

To further determine the form under which the FBNSV crosses the cellular barriers within its aphid vector, we compared the localization of the FBNSV DNA to that of the two viral proteins obviously involved in vector transmission, CP and NSP. First, we looked at the localization of the CP using immunofluorescence (IF). The CP exhibited a distribution identical to that of viral DNA with very numerous cytoplasmic fluorescent foci in AMG cells (**Figure 4A**). In PSG, CP-associated fluorescent foci were visible in cells of type-4, just as viral DNA, but also in the cells with the biggest nucleus, defined by Ponsen as the type-3 cells (**Figure 4E and Figure 2C**). We then used a combination of FISH and IF to more precisely co-localize viral genomic DNA and CP. In the AMG, this DNA/protein co-labeling demonstrated

that all intracellular foci containing viral DNA also contained the CP (**Figure 4I & J)**, consistent with the assumption that nanoviruses circulate from the infected plant sap, through gut cells into the hemolymph and through salivary gland cells into the saliva, as mature virus particles (26). Noticeably, some smaller CP aggregates appeared sometimes visible in the absence of labeling of the viral DNA. In the PSG, probably due to much weaker fluorescent signals (see Discussion), we could not observe a reliable FISH/IF double signal and so the co-localization of viral DNA and CP could not be confirmed in this tissue.

The same approach was applied to NSP, which was first labeled through IF alone. In both AMG and PSG, the distribution of the NSP-associated fluorescent foci was similar to that observed for the CP (**Figure 4C and G**). Combining FISH and IF, we then co-labeled NSP and viral DNA in AMG cells. As observed for CP, the intracellular foci containing FBNSV DNA appeared to contain the NSP protein as well (**Figure 4K & L**). However, a strong heterogeneity in the relative intensity of the signals respectively attributable to viral DNA and NSP was observed among distinct aggregates of the same cells (**Figure 4K, see graph**), and is discussed further below. This result indicates that both virus particles and NSP likely follow the same pathway during entry and accumulation within insect cells. Unfortunately, the lack of specific antibodies that would be produced in distinct animal species precluded direct colocalization assays of NSP and CP.

FBNSV needs NSP to accumulate in AMG cells

To pave the way to the future deciphering of the NSP mode of action, we questioned whether this protein is mandatory for viral accumulation in AMG cells. Earlier work investigating the dependency of FBNSV infection on the presence/absence of individual genome segments (24) demonstrated that the absence of U4 does not affect systemic infection of host plants nor aphid-transmission from these plants. In contrast, the absence of segment N does not affect infection but totally abolishes aphid transmission. We thus assessed whether FBNSV could accumulate within AMG cells when acquired from source plants infected with FBNSV wild-type, FBNSV lacking segment U4, FBNSV lacking segment N, or a FBNSV mutant where the start codon of the protein NSP in the segment N has been suppressed through mutagenesis. FISH observation showed no difference in the viral DNA accumulation pattern within AMG cells of aphids fed on plants containing or lacking segment U4 (**Figure 5A and B**). In contrast, the absence of segment N in infected plants totally abolished the accumulation of the viral genome in AMG cells (**Figure 5C**). Similarly, the absence of accumulation of the viral genome in aphids fed on plants infected with the ATG-mutated N segment (**Figure 5D**) confirmed that it is the protein NSP that is mandatory for FBNSV accumulation within vector gut cells rather than the segment N itself.

Modifications at N- or C-terminus of NSP alter its function or stability

Because it would be easier to further characterize NSP derivatives fused to small purification tag, we modified the sequence of segment N in order to introduce a series of 6 histidines either at the N- (His-NSP) or C-terminus (NSP-His) of the NSP protein. Plants were infected with either of these constructs and PCR detection confirmed the maintenance of the modified versions of segment N during systemic plant infection (**Figure 5E**). However, while the His-NSP fusion protein accumulated to a level comparable to wild type NSP in infected plant tissues, NSP-His could not be detected (**Figure 5E**). The failure to detect NSP-His fusion could be due to instability of the modified protein or mRNA, or to other unknown reasons.

To assess the functionality of the His-NSP fusion produced in infected plants, we tested whether aphids could acquire and transmit the virus from these plants (**Figure 5F to I**). FISH and IF respectively showed that no viral DNA nor His-NSP fusion accumulated detectably in AMG cells. Consistently, in two repeated experiments, aphids that acquired FBNSV from infected plants expressing His-NSP failed to transmit (no infected plants out of 95 test plants; see Materials and Methods for details), while aphids fed on infected plants expressing wild type NSP efficiently transmitted the virus (69 infected plants out of 105 test plants).

All together these results indicate that modification at the N- or C-terminus of NSP have profound effects on accumulation and/or functionality of this protein in aphid vectors and further confirm that only functional NSP can enter gut cells and assist the co-entry of the CP and viral genome.

Discussion

The route of FBNSV in its vector *A. pisum*

Because very few experimental data are available concerning the cellular and molecular interactions between nanoviruses and their aphid vectors, we investigated it anew on the model species *Faba bean necrotic stunt virus* transmitted by *Acyrthosiphon pisum*. The first logical step was to precisely localize the distinct viral components that are required for successful transmission: viral genomic DNA, coat protein and helper component NSP. Using FISH and IF to monitor these three viral components, we can definitely confirm that FBNSV specifically accumulates in the AMG and PSG, consistent with a circulative non-propagative mode of transmission. This observation matches the reported localization of the coat protein of BBTV in its aphid vector *P. nigronervosa* (17). FBNSV and BBTV respectively belong to the

genus *Nanovirus* and *Babuvirus*, the only two genera of the family *Nanoviridae*. It is thus most likely that the aphid AMG and PSG are the organs specifically involved in the transmission of all nanoviruses. This within-vector route is similar to that of geminiviruses transmitted by whiteflies (27) but contrasts with that of luteoviruses which can enter and cross cells of the hindgut (7-9) and have only been reported in accessory salivary glands of their aphid vectors (9).

In the PSG, FBNSV DNA was unambiguously detected solely in type-4 cells whereas CP and NSP proteins were detected both in type-4 and type-3 cells. At this point, because we do not have sound biological arguments that could explain the accumulation of viral coat protein and not DNA, we assume that the lack of detection of viral DNA in type-3 cells is due to a technical bias where the fluorescent signal associated to FISH is weaker than that associated to IF. In any case, it will be interesting to further investigate the specific accumulation of FBNSV in PSG cells over time, as previously reported for a begomovirus in its whitefly vector (28). At this point, we cannot exclude that FBNSV could penetrate other cell types and later accumulate preferentially in cell types 3 and 4.

Intracellular localization of FBNSV

FBNSV is a ssDNA virus encoding a replication protein M-Rep that is not a DNA polymerase (29). On the basis of inference from data obtained from related geminiviruses, nanoviruses are thought to recruit a non-identified cellular DNA polymerase for replication and accumulation in the nucleus of host plant cells (20). Within aphid vectors, we observed a cytoplasmic localization of FBNSV DNA and proteins, supporting the absence of replication. This result must be considered with care, however, because the question of viral replication within the vector has long been a matter of controversy in the related family *Geminiviridae* (30, 31). TYLCV primarily accumulates in the cytoplasm of AMG and PSG of its whitefly vector (28), but an elusive transient replication phase has nevertheless been evidenced soon after acquisition (30). In the present study, we used aphids that were all allowed a very long acquisition access period, in order to maximize the detection of viral material accumulated in the cytoplasm of AMG and PSG over time. A small “transient replicative” proportion of the viral DNA could eventually remain overlooked under our experimental conditions. We have earlier reported that the FBNSV genome formula (the relative amounts of each FBNSV genome segments) changes when the virus passes from the infected plant into the aphid vector (32). Among other hypotheses, replication of the virus upon entry into insect cells could explain the formula changes, and so the question of a transient replication phase of FBNSV within its aphid vector remains open.

Vesicles of the endosomal pathway have been suggested to be the entry route of luteoviruses and geminiviruses in their vectors, through electron microscopy in viruliferous aphids (9) and through colocalization with markers of cell organelles and confocal microscopy in viruliferous whiteflies (11). An earlier attempt with markers of subcellular compartments to identify the accumulation sites of the nanovirus BBTV failed (19). The authors suggested that this failure could be due to the lack of markers specifically adapted to aphids. For this reason, we have not identified the subcellular compartment with which the FBNSV associates during transcytosis. Developing a large panel of aphid/whitefly-specific markers will be of great utility because the endocytosis/exocytosis pathways that are used downstream of the early endosome remains unknown for the three viral families.

The DNA and coat protein perfectly co-localized in the cytoplasmic fluorescent foci, supporting the general assumption that the FBNSV goes across cellular barriers of its aphid vector under the form of mature virus particles. A remarkable fact inspires caution, however. For both begomoviruses and nanoviruses no distinctive virus particles could ever be visualized within any cell of an insect vector through electron microscopy. For luteoviruses, which are not much bigger (≈25 nm in diameter), images of virions within intracellular vesicles have long and repeatedly been published (9, 33-35). The reason precluding analogous images with begomo- and nanoviruses is intriguing. While co-localization of DNA and coat protein indicates that the two travel together, it does not represent a definitive proof that they do so as assembled virus particles.

Role of NSP in the transmission of FBNSV

Franz and collaborators (23) demonstrated the requirement of a helper component (HC) for aphid-transmission of faba bean necrotic yellows virus (FBNYV). Nearly two decades later, the same research group (23) demonstrated that this HC is the viral protein NSP encoded by the N segment. HC molecules have been reported mostly in cases of non-circulative transmission, the best-known examples being caulimoviruses and potyviruses (4). In these cases, the HC creates a reversible molecular bridge between the virus and the insect mouthparts, a phenomenon called the “bridge hypothesis” (36), with one domain interacting with the viral coat protein (37, 38) and another with receptor molecules of the vector (39-41). HCs had not been reported until recently in circulative transmission, either propagative or not. With the discovery that the rice stripe tenuivirus (RSV) (42) and FBNSV (24) have also evolved the use of a HC, the so-called “helper strategy” (36) is now found in all types of virus/vector interactions. In the case of RSV, the HC is a virus-encoded glycoprotein that binds to the CP and mediates endocytosis and entry of the virus particles inside gut cells. Here, we similarly demonstrate that the NSP protein of FBNSV

300 is mandatory for viral accumulation within AMG cells, and thus presumably for virus entry within the
301 vector. We further show that NSP localizes, though imperfectly, in the same intracellular aggregates as
302 viral DNA and we can thus hypothesize that FBNSV transits within aphids as virus particle-NSP
303 macromolecular complexes. These observations suggest that HCs have at least partly similar mode of
304 action in non-circulative and in circulative transmission: creating a molecular bridge between virus and
305 vector. The imperfect co-localization observed for NSP and viral DNA, however, may indicate a distinct
306 and unknown mode of action and we believe further investigation is needed to confirm or refute the
307 bridge hypothesis. While the NSP of the *Babuvirus* BBTV has been shown to bind CP (43, 44), the
308 requirement of this interaction for successful transmission is not demonstrated. Likewise, a direct
309 binding of NSP to the cellular membranes in the AMG lumen and the identification of a putative specific
310 receptor at this site await further research effort. Unfortunately, investigation on the mode of action of
311 NSP can be foreseen as a difficult task because our results demonstrate that modifications of NSP N- or
312 C-termini to produce protein-fusions amenable to biochemical approaches leads to very low
313 accumulation of the recombinant protein or to a loss of its biological activity.

314 **All FBNSV genome segments co-localize within individual cells of the aphid vector**

315 It is generally assumed that the multipartite lifestyle entails an important cost related to the probability
316 of losing genome segments during transmission from cell-to-cell or host-to-host (21, 45, 46). For highly
317 multipartite viruses -i.e. with a genome composed of 4 or more segments- the multiplicity of infection
318 (MOI) theoretically required for these viral systems to evolve has been predicted to be unrealistically
319 high (21, 47). We have recently demonstrated that FBNSV can infect its host plant with its distinct genes
320 (genome segments) separated in distinct cells, by exchanging gene products across these cells (22). This
321 capacity allows infection of plant cells at very low MOI, likely alleviating the cost of the multipartite
322 lifestyle within host. In the present work we touch on the mechanisms through which all FBNSV
323 segments may be transmitted between hosts. Obviously, the FBNSV massive accumulation in aphid cells
324 is totally different from the low MOI infection observed in plant cells (see the striking contrast in figures
325 2G and H). All susceptible cells of the AMG are packed with all genome segments. Although we did not
326 formally quantify it, one can easily observe that each AMG cell contains hundreds of fluorescent foci. By
327 using different pairs of segment-specific probes, we established that each of these foci systematically
328 contains the two segments tested. This indicates that each focus contains numerous distinct segments
329 and most probably all eight. We can thus conservatively conclude that several hundreds to thousands of
330 virus particles enter and accumulate over time within each cell of the AMG. In the PSG, the fluorescent

signal was weaker with some foci eventually containing a dominant color (so perhaps only one segment of the tested pair), indicating a reduction of the number of viral particles accumulated in this organ. It is likely that, as described for geminiviruses (48), FBNSV is primarily stored in AMG and slowly released into the hemolymph to reach the salivary glands and from there the saliva. The success of each genome segment during this transit and after inoculation into new plants is uncertain, since the probability of successful transmission by individual aphids is ~40% (47); the transmission failures could potentially be due to the lack of successful transmission of all genomic segments. It is conceivable that, on the one hand, a low viral flow from the "AMG viral stock" through salivary glands allows viruliferous aphids to release viral particles and to possibly transmit during their whole lifespan. On the other hand, the much weaker virus accumulation in the salivary glands suggests that the number of viral particles released in each new visited plant is such small that single aphids often fail to transmit. We cannot quantify precisely the number of virus particles in the salivary glands, but this weaker accumulation is at least qualitatively compatible with the very low numbers of copies of each segment estimated to be transmitted by aphids during host-to-host transmission (47).

Materials and Methods

Virus isolate and clones, host plant and aphid colony

The FBNSV was first isolated from faba bean in Ethiopia 1997 (49) and then characterized in 2009 (50). Each of the 8 FBNSV genome segments encodes only one protein: segment C encodes the cell cycle-linked protein (Clink), M encodes the movement protein (MP), N encodes the nuclear-shuttle protein (NSP), S encodes the coat protein (CP), R encodes the master-replication associated protein (M-Rep) and U1, U2 and U4 encode proteins of unknown functions (**Figure 1**). Each genome segment of this isolate has been inserted as an head-to-tail dimer into the binary plasmid pBin19 to create eight plasmids together constituting the FBNSV infectious clone (50).

With the aim to purify an active NSP protein derivative, we added an hexa-histidine (His) tag at the C- or N-terminus of this protein using the Q5® site-directed mutagenesis kit (NEB). The plasmid encoding NSP-His was constructed by inserting the sequence $^{5'}$CATCATCATCACCACCAC$^{3'}$ just before the stop codon of the coding sequence of the DNA-N (Genbank Acc. No. GQ150782) in the plasmid pCambia 2300-N-SL (51), to generate pCambia 2300-N-His-SL. The plasmid encoding His-NSP was constructed by inserting the same sequence immediately after the initiating ATG of DNA-N in pCambia 2300-N-SL to generate

pCambia 2300-His-N-SL. The sequences of the primers used for these two constructs are listed in **Table 1**. We refer to these NSP proteins his-tagged at their C- or N-terminus as NSP-His and His-NSP, respectively. The correct insertion of the series of six histidine codons was confirmed by Sanger sequencing. Plasmids pCambia 2300-N-His-SL and pCambia 2300-His-N-SL were finally transferred to *Agrobacterium tumefaciens* COR308 for subsequent agroinoculation in faba bean host plants.

Faba bean (*Vica faba*, cv. "Sevilla", Vilmorin) was used as the host plant in all agro-inoculation experiments. Ten days-old plantlets were agro-inoculated with the FBNSV infectious clone as described (50). In some cases the complete set of 8 cloned segments was used, and in other cases either the cloned segment N or U4 was omitted. Faba beans were maintained in growth chambers under a 13/11 hours day/night photoperiod at a temperature of 26/20°C day/night and 70% hygrometry. The soil of each potted plant was treated with a solution of 2 g Trigard 75 WP (Syngeta® - ref: 24923) in 5 L of water to avoid the development of sciarid flies. All FBNSV-infected plants were analyzed by qPCR to control for the presence/absence of each inoculated segment.

Aphid colonies of *Acyrthosiphon pisum* (clones 210 and LSR1) were reared on either FBNSV-infected ("viruliferous aphids") or healthy ("non-viruliferous aphids") plants. Every week, aphids were transferred to new plants and the colonies were maintained under a 16/8 hours day/night photoperiod at a temperature of 23/18°C day/night.

For practical space reasons, pea (*Pisum sativum*, cv. "Provencal", Vilmorin) was used as the recipient plant during transmission experiments.

Preparation of aphid midguts and salivary glands

To facilitate the dissection and to get insects with an important virus load, we used adult aphids from the colony maintained on infected plants. To eliminate the virus present in the lumen of the gut, aphid individuals were "purged" by a 24 hours acquisition access period on water through Parafilm membrane as described (52). Guts and salivary glands of aphids were dissected in PBS 1X (pH 7.4) and fixed in paraformaldehyde 4% prepared in PBS 1X for 20 minutes. Dissected organs were then incubated in 0.1 M glycine pH 7.4 for at least 15 minutes in order to stop the fixation reaction. For posterior FISH treatments, samples were then submitted to a discoloration step of 20 min in 30% H_2O_2, and kept in PBS 1X at 4°C until use (maximum storage time: 3 weeks). When applying IF to the samples, either alone or in combination with FISH, this discoloration step was omitted.

Fluorescent in situ hybridization (FISH) and immunofluorescence (IF)

Fluorescent DNA probes specific to each of the eight FBNSV segments were prepared exactly as described in (22, 53). Briefly, the coding sequence of each FBNSV segment was first amplified by PCR. PCR products from individual segments or a mixture thereof were then used as templates for the probe synthesis by random priming and incorporation of Alexa Fluor-labeled dUTP, using the BioPrime DNA labeling system kit (Invitrogen). The primer pairs used to amplify the coding sequence of each segment were those described in (22). For segment-specific labeling, amplified coding sequences of C, M, R or U2 were labeled with Alexa fluor 488 (green) and those of N, S, U1 or U4 with Alexa fluor 568 (red). For detection of FBNSV DNA, organs kept in PSB 1X were rinsed three times during 5 minutes in hybridization buffer (20 mM Tris-HCl pH8, 0.9 M NaCl, 0.01% SDS and 30% formamide) (54) and then incubated with the fluorescent probes (diluted 1/30 in hybridization buffer) overnight at 37°C. Labeling was stopped by three rinses in hybridization buffer followed by one rinse in PBS 1X. Samples were mounted on microscope slides in Vectashield® antifade mounting medium (Vector Laboratories) (22) and observed with a Zeiss LSM700 confocal microscope equipped with X10, X20, X40 or X63 objectives.

For localization of the coat protein, we used a mix of three previously described (50, 55) mouse monoclonal antibodies (FBNYV-1-1F2, FBNYV-2-1A1 and FBNYV-3-4F2). This mix was named FBNSV-FBNYV anti-CP and used at a 1/200 dilution. For detection of the protein NSP, we used the mouse monoclonal antibody FBNSV-NSP Mab 1-3G9 (24) diluted 1/200. Dissected anterior midgut (AMG) and salivary gland (SG) samples were incubated 10 minutes with 1 µg/µL of proteinase K (PK) to increase the tissue “permeability” (56). Then, samples were rinsed three times 5 min in 0.1 M glycine pH 7.4 and twice in PBS 1X to stop the PK treatment, and a second fixation was performed in PFA 2 %. After this second PFA fixation, we incubated the organs in a PBS 1X + 5% BSA solution during 1 h and 30 min to saturate the non-specific fixation sites. Then, AMG and SG were incubated with the primary antibody in PBS 1X + 5% BSA overnight at 4°C and with the secondary antibody (goat anti-mousse Alexa Fluor 594 IgG conjugate, diluted 1/250, Life Technologies) in PBS 1X + 5% BSA during 1 h at 37°C. After each antibody incubation, three rinses in PBS 1X + Triton 0.2 % (0.2 % PBST) were perform. The samples were mounted on microscope slides. All images were taken at a resolution of 512 X 512 or 1024 X 1024 pixels.

When combining FISH and IF on the same samples, after initial fixation in PFA 4%, PK treatment was carried out before FISH labeling which was always applied prior to IF. We used ImageJ software version 1.4.3.67 to analyze images. The overall intensity of green, red and blue signals was adjusted for each image as described in (22).

Transmission tests with the mutated NSP

Faba bean plantlets were agro-inoculated with the 7 wild-type plasmids of the FBNSV infectious clone: C, M, R, S, U1, U2 and U4, plus either pCambia 2300-N-His-SL or pCambia 2300-His-N-SL. After 21 days (21 dpi), plants were tested by PCR or qPCR (see details in next section) for the presence of the complete set of segments. Production of NSP-His or His-NSP protein in infected plants was controlled by Western blot (WB). A piece of 0.6 g of an infected plant stem was finely ground in liquid nitrogen using a mortar. Then, the powdered tissue was further homogenized in 1800 µL of extraction buffer (Tris-HCl 20 mM, Na_2SO_3 0.2 % and SDS 0.2 %) maintained on ice. The resulting crude extract was incubated under agitation at room temperature for 20 minutes and at 4°C for 1 hour, prior to centrifugation at 8000 g for 15 minutes. Twenty microliters of supernatant were used for the WB analysis. As primary antibody we used either the rabbit FBNSV IgG 1511389 C-ter - anti-NSP antibody (produced from the NSP peptide sequence: C-QYLKKDEDYRRKFII) or a mouse 6X-His tag antibody (Invitrogen). The secondary antibody was an anti-mouse or -rabbit IgG coupled with phosphatase alkaline (produced in goat - Sigma). Finally, the membrane was revealed in a solution containing the phosphatase alkaline substrate (BCIP 0.15 mg/ml, NBT 0.30 mg/ml, Tris buffer 100 mM and $MgCl_2$ 5 mM at pH 9.25-9.75 - Sigma).

Aphids reared on plants inoculated with plasmids pCambia 2300-N-His-SL or pCambia 2300-His-N-SL were used to observe the localization of the NSP protein derivatives in AMG and for transmission testing. For transmission tests, L1 stage larvae were deposited on infected faba bean plants for an acquisition access period (AAP) of 3 days, and transferred to healthy pea plantlets for an inoculation access period (IAP) of 3 days. Aphids were then killed with insecticide (Pirimor – Certis® – 1 g/L in water) and plants were observed for the appearance of symptoms 21 days after inoculation. Three experiments were ran in parallel, one with plants infected with the eight wild-type segments and the other two with plants infected with seven wild-type segments and either pCambia 2300-N-His-SL or pCambia 2300-His-N-SL.

DNA extraction and quantitative real-time PCR

Extraction of total DNA from healthy or FBNSV-infected plants was performed using three leaf disks (0.6 cm each) from the two upper leaf levels squashed onto a Whatman paper. The corresponding piece of Whatman paper was then placed into a 200 µL filter tip. 100 µL of modified Edwards buffer (200 mM Tris-HCl pH 7.5, 25 mM EDTA, 250 mM NaCl, 0.5% SDS, 1% PVP40, 0.2% ascorbic acid) were added to the Whatman paper disk, and the filter tip was placed on the top of a PCR plate and centrifuged at 5000 g for 15 seconds. One hundred microliters of isopropanol were added to the liquid recovered down in the well

of the PCR plate and further centrifuged 25 min at 5000 g. The supernatant was discarded and the pellet was washed with 100 µL of ethanol 70 % and resuspended in 50 µL of distilled water.

Total DNA was extracted from pools of five dissected heads or bodies of viruliferous aphids, as previously described (32). Twenty pools were used to qPCR-estimate the average number of copies of the 8 FBNSV genome segments accumulating in each of these body parts. qPCR was carried out on a LightCycler 480 thermocycler (Roche) The LightCycler FastStart DNA Master Plus SYBR green I kit (Roche) was used according to the manufacturer's instructions using 5 µL of the 2X qPCR Mastermix, 2.5 to 2.7 µl of H_2O, 0.3 to 0.5 µl of the primer mixes (depending of the primers – 0.3 µM final for C, M and S and 0.5 µM final for the other segments), and 2 µL of DNA sample (diluted 10-fold in H_2O) as matrix. The FBNSV pair of primers used have been described in (57). Forty qPCR cycles of 95°C for 10 s, 60°C for 10 s and 72°C for 10 s were applied to the samples. Post-PCR data analysis were as described (58). The plant extracts were also tested by standard PCR when verifying the presence of the his-tag coding sequence in the segment N, using specific primer pairs (**Table 1**).

Acknowledgments

We are grateful to B. Gronenborn, T. Timchenko and J. Vetten for providing antibodies against the CP and NSP of FBNSV. We acknowledge the precious help of S. Leblaye for all plant production and aphid maintenance, as well as for agro-inoculation of FBNSV infectious clone. This work was supported by ANR Grants N°ANR-14-CE02-0014-01 and ANR-18-CE92-0028-01. JD acknowledges support from the University of Montpellier; SB, MY, MSV, EP and MV from INRA-SPE; JLZ and YM from IRD; YM from CNRS, YG and HZ from JKI Braunschweig Germany.

Figure legends

Figure 1: Genome organization of *Faba bean necrotic stunt virus* (FBSNV). The eight circles represent the different genomic segments. The name and size of each genome segment and the name of the encoded protein are indicated inside circles in black and green, respectively. Clink, Cell-cycle linked protein; MP, movement protein; NSP, nuclear shuttle protein; M-Rep, master rep; CP, coat protein; U1, U2 or U4, unknown protein 1, 2 or 4. CR-SL: common stem loop region; CR-II: common region; ORF: open reading frame.

Figure 2: Localization of the DNA segments of *Faba bean necrotic stunt virus* (FBSNV) in aphid *vs* plant cells. Schematic drawing of the anatomy of the AMG (A) shows longitudinal (Ai) and transversal sections (Aii-Aiv). Schematic drawing of the anatomy of the salivary glands (D) shows longitudinal sections of the accessory (Di) and principal glands (Dii) as well as transversal sections of the principal glands (Diii & Div). Both A and D are adapted from Ponsen (25) describing the anatomy of *Myzus persicae*. Ponsen's numbering of distinct cell types (1 to 8) of the salivary glands is indicated in D. The accumulation of FBNSV DNA was observed in 64 viruliferous aphid's anterior midgut (AMG) from 8 experiments, and a representative image is shown in (B). The accumulation of FBNSV DNA in a specific cell type of the principal salivary glands (PSG) was observed in 15 viruliferous aphids from 3 experiments and a representative image is shown in (E). In B and E, the viral DNA is revealed by FISH (green probe targeting all 8 FBNSV segments) and non-viruliferous controls are shown in C and F. The respective localization of R and S segments (probe color as indicated) is compared in AMG cells (G, representative of 24 observed aphids) and in infected faba bean phloem cells (H, see also ref N° 22). The respective localization of U2 and U4 segments is compared in PSG cells (I, representative of 4 aphids observed). In G, H, and I, the merge color channel image is shown at the bottom and the corresponding split color channel images are shown at the top. All images correspond to maximum intensity projections. Cell nuclei are DAPI-stained in blue. pmg: posterior midgut; asg: accessory salivary glands.

Figure 3: Co-localization of FBNSV segments in AMG and PSG. The color of the fluorescent probes and the targeted segment pairs are indicated. Three additional pairs of segments have been tested in the AMG: 32 aphids from 4 experiments for the pair M/U1, and 24 aphids from 3 experiments for the pairs C/N and U2/U4, and illustrative images are respectively shown in A, B and C. In the PSG, the additional

segment pair M/U1 was observed in 6 aphids from 3 experiments and a representative image is shown in (D). Split color channels are shown on the left and middle panels whereas merges are shown on the right. All images correspond to maximum intensity projections. Cell nuclei are DAPI-stained in blue.

Figure 4: Localization of FBNSV DNA, CP and NSP proteins in AMG and PSG of *A. pisum*. FBNSV CP is labeled by IF in AMG (A and B) and PSG (E, F) of viruliferous (A, E) and non-viruliferous aphids (B, F). NSP is labeled by IF in AMG (C, D) and PSG (G, H) of viruliferous (C, G) and nonviruliferous aphids (D, H). When co-labeling viral DNA and either CP or NSP (FISH + IF) in AMG, the DNA probe is targeting all eight genome segments and shines green whereas the specific CP or NSP antibody shines red (I to L). In each case, 30 aphids from 3 experiments were observed and one representative image is shown. Split color channel images in I and K correspond to merged color channel images J and L, respectively. The graphics represent the co-localization profiles between either DNA (green curve) and CP (red curve) (I) or DNA (green curve) and NSP (red curve) (K). Fluorescence intensity was measured along the white arrow drawn in J and L. Images A to H correspond to maximum intensity projections and images I to L correspond to single optical sections. Cell nuclei are DAPI-stained in blue.

Figure 5: NSP-dependent accumulation of FBNSV DNA in the AMG of aphid vector. FBNSV DNA is green-labeled in gut cells of aphids fed either on infected plants containing all FBNSV segments (A, representative of 15 aphids from 3 experiments), or on infected plants lacking segment U4 (B, representative of 5 aphids from 1 experiment), or on infected plants lacking segment N (C, representative of 15 aphids from 3 experiments), or on infected plants with all 8 segments but where the N segment has a mutation of the ATG-start codon (D, representative of 5 aphids from 1 experiment). The presence of the N segment and derivatives His-N and N-His in two replicate infected plants is verified by PCR using primers specific of the coding sequence of the his-tag (E, top panel). The expression of NSP, His-NSP and NSP-His proteins in infected plant tissues is evaluated by Western blot (E) using antisera directed against NSP (middle panel) or his-tag (bottom panel). FBNSV NSP (F and G, red) or DNA (H and I, green) are labeled in aphids fed on infected plants expressing wild type NSP (F and H) or its derivative His-NSP fusion (G and I). Images F and H are both representative of 20 aphids observed from 2 experiments. All confocal images are maximum intensity projections. Cell nuclei are DAPI-stained in blue.

533 T**able 1:** List of primers

	Target DNA	Forward (5' → 3')	Reverse (5' → 3')
FISH[a]	C	ATGGGTCTGAAATATTTCTC	TTAATTAATTACAATCTCC
	M	GCTGCGTATCAAGACGAC	TTCTAGCATCCCAATTCCTTTC
	N	TGGCAGATTGGTTTTCTAGT	TTCTGAGTGAATGTACAATAAACATTT
	R	ACATTAAATAATCCTCTCTCTCCTA	CCTATCATCACTAAACATGCC
	S	AAATGGTGAGCAATTGGAA	GCCTATGATAGTAATCATATCTTGACA
	U1	TTGGTCGATTATTTGTTGGTT	AATATCTCATTAGCATTAATTACATTTGAA
	U2	TTATGGATGCCGGCTTT	CATCAAGTATTAGAATAACGAACTTGA
	U4	AGCAGGTTATCGAATGTAG	ATAGATTCCCACAATCGCT
Mutagenesis[b]	N-His	CACCACCACGCAGATTGGTTTTCTAGTC	ATGATGATGCATTTTTCTGCAACTTCC
	His-N	CACCACCACTAATTAGTTGTGATGATGTAATTAATAATAATT	ATGATGATGCACTTTGATTCTGAGTGAATG
Control His[c]	ATG-His	ATGCATCATCATCACCACCAC	GTTCCTGTTTCCACCATAGAAACTAC
	His-TAA	GCATGAAAGACAAGCTCAACG	TTAGTGGTGGTGATGATGATG

534

535 [a] Primer pairs used to amplify the coding sequence of each segment for segment-specific fluorescent
536 labeling during FISH experimentation

537 [b] Primer pairs used to generate the pCambia 2300-His-N-SL or pCambia 2300-N-His-SL.

538 [c] Primer pairs used to control the presence of DNA-His-N or DNA-N-His in infected plants

539

References

1. 1. **Hogenhout SA, Ammar el D, Whitfield AE, Redinbaugh MG.** 2008. Insect vector interactions with persistently transmitted viruses. Annu Rev Phytopathol **46:**327-359.
2. **Ng JC, Perry KL.** 2004. Transmission of plant viruses by aphid vectors. Mol Plant Pathol **5:**505-511.
3. **Nault LR.** 1997. Arthropod transmission of plant viruses : a new synthesis. Ann Entomol Soc Am **90:**521-541.
4. **Blanc S, Drucker M, Uzest M.** 2014. Localizing viruses in their insect vectors. Annu Rev Phytopathol **52:**403-425.
5. **Blanc S, Gutierrez S.** 2015. The specifics of vector transmission of arboviruses of vertebrates and plants. Curr Opin Virol **15:**27-33.
6. **Gray S, Cilia M, Ghanim M.** 2014. Circulative, "nonpropagative" virus transmission: an orchestra of virus-, insect-, and plant-derived instruments. Adv Virus Res **89:**141-199.
7. **Gray SM, Gildow FE.** 2003. Luteovirus-aphid interactions. Annu Rev Phytopathol **41:**539-566.
8. **Reinbold C, Herrbach E, Brault V.** 2003. Posterior midgut and hindgut are both sites of acquisition of Cucurbit aphid-borne yellows virus in Myzus persicae and Aphis gossypii. J Gen Virol **84:**3473-3484.
9. **Brault V, Herrbach E, Reinbold C.** 2007. Electron microscopy studies on luteovirid transmission by aphids. Micron **38:**302-312.
10. **Ali M, Anwar S, Shuja MN, Tripathi RK, Singh J.** 2018. The genus luteovirus from infection to disease. Eur J Plant Pathol **151:**841-860.
11. **Xia WQ, Liang Y, Chi Y, Pan LL, Zhao J, Liu SS, Wang XW.** 2018. Intracellular trafficking of begomoviruses in the midgut cells of their insect vector. PLoS Pathog **14:**e1006866.
12. **Linz LB, Liu S, Chougule NP, Bonning BC.** 2015. In Vitro Evidence Supports Membrane Alanyl Aminopeptidase N as a Receptor for a Plant Virus in the Pea Aphid Vector. J Virol **89:**11203-11212.
13. **Tang SL, Linz LB, Bonning BC, Pohl NL.** 2015. Automated Solution-Phase Synthesis of Insect Glycans to Probe the Binding Affinity of Pea Enation Mosaic Virus. J Org Chem **80:**10482-10489.
14. **Mulot M, Monsion B, Boissinot S, Rastegar M, Meyer S, Bochet N, Brault V.** 2018. Transmission of Turnip yellows virus by Myzus persicae Is Reduced by Feeding Aphids on Double-Stranded RNA Targeting the Ephrin Receptor Protein. Front Microbiol **9:**457.

15. **Wang LL, Wang XR, Wei XM, Huang H, Wu JX, Chen XX, Liu SS, Wang XW.** 2016. The autophagy pathway participates in resistance to tomato yellow leaf curl virus infection in whiteflies. Autophagy **12:**1560-1574.
16. **Vetten HJ, Dale JL, Grigoras I, Gronenborn B, Harding R, Randles JW, Thomas JE, Timchenko T and Yeh HH.** *Nanoviridae* p 395-404. 2011. in King AMQ, Lefkowitz EJ, Adams MJ, Carstens EB,(ed), Elsevier, Virus taxonomy: the classification and nomenclature of viruses: the 9th report of the ICTV. AP press.
17. **Bressan A, Watanabe S.** 2011. Immunofluorescence localisation of Banana bunchy top virus (family Nanoviridae) within the aphid vector, Pentalonia nigronervosa, suggests a virus tropism distinct from aphid-transmitted luteoviruses. Virus Res **155:**520-525.
18. **Watanabe S, Bressan A.** 2013. Tropism, compartmentalization and retention of banana bunchy top virus (Nanoviridae) in the aphid vector Pentalonia nigronervosa. J Gen Virol **94:**209-219.
19. **Watanabe S, Borthakur D, Bressan A.** 2016. Localization of Banana bunchy top virus and cellular compartments in gut and salivary gland tissues of the aphid vector Pentalonia nigronervosa. Insect Sci **23:**591-602.
20. **Gronenborn B.** 2004. Nanoviruses: genome organisation and protein function. Vet Microbiol **98:**103-109.
21. **Iranzo J, Manrubia SC.** 2012. Evolutionary dynamics of genome segmentation in multipartite viruses. Proc Biol Sci **279:**3812-3819.
22. **Sicard A, Pirolles E, Gallet R, Vernerey MS, Yvon M, Urbino C, Peterschmitt M, Gutierrez S, Michalakis Y, Blanc S.** 2019. A multicellular way of life for a multipartite virus. Elife **8:**e43599.
23. **Franz AW, van der Wilk F, Verbeek M, Dullemans AM, van den Heuvel JF.** 1999. Faba bean necrotic yellows virus (genus Nanovirus) requires a helper factor for its aphid transmission. Virology **262:**210-219.
24. **Grigoras I, Vetten HJ, Commandeur U, Ziebell H, Gronenborn B, Timchenko T.** 2018. Nanovirus DNA-N encodes a protein mandatory for aphid transmission. Virology **522:**281-291.
25. **Ponsen MB.** 1972. The site of potato leafroll virus multiplication in its vector, Myzus persicae: an anatomical study. Meded Landbouwhogesch Wageningen **72:**1-147.
26. **Whitfield AE, Falk BW, Rotenberg D.** 2015. Insect vector-mediated transmission of plant viruses. Virology **479-480:**278-289.
27. **Czosnek H, Hariton-Shalev A, Sobol I, Gorovits R, Ghanim M.** 2017. The Incredible Journey of Begomoviruses in Their Whitefly Vector. Viruses **9:**e273.

28. **Wei J, Zhao JJ, Zhang T, Li FF, Ghanim M, Zhou XP, Ye GY, Liu SS, Wang XW.** 2014. Specific cells in the primary salivary glands of the whitefly Bemisia tabaci control retention and transmission of begomoviruses. J Virol **88:**13460-13468.

29. **Timchenko T, de Kouchkovsky F, Katul L, David C, Vetten HJ, Gronenborn B.** 1999. A single rep protein initiates replication of multiple genome components of faba bean necrotic yellows virus, a single-stranded DNA virus of plants. J Virol **73:**10173-10182.

30. **Pakkianathan BC, Kontsedalov S, Lebedev G, Mahadav A, Zeidan M, Czosnek H, Ghanim M.** 2015. Replication of Tomato Yellow Leaf Curl Virus in Its Whitefly Vector, Bemisia tabaci. J Virol **89:**9791-9803.

31. **Sanchez-Campos S, Rodriguez-Negrete EA, Cruzado L, Grande-Perez A, Bejarano ER, Navas-Castillo J, Moriones E.** 2016. Tomato yellow leaf curl virus: No evidence for replication in the insect vector Bemisia tabaci. Sci Rep **6:**30942.

32. **Sicard A, Zeddam JL, Yvon M, Michalakis Y, Gutierrez S, Blanc S.** 2015. Circulative Nonpropagative Aphid Transmission of Nanoviruses: an Oversimplified View. J Virol **89:**9719-9726.

33. **Harris KF, Bath JE.** 1972. The fate of pea enation mosaic virus in its pea aphid vector, Acyrthosiphon pisum (Harris). Virology **50:**778-790.

34. **Garret A, Kerlan C, Thomas D.** 1993. The intestine is a site of passage for potato leafroll virus from the gut lumen into the haemocoel in the aphid vector, Myzus persicae Sulz. Arch Virol **131:**377-392.

35. **Gildow F.** 1993. Evidence for receptor-mediated endocytosis regulating luteovirus acquisition by aphids. Phytopathology **83:**270-277.

36. **Pirone TP, Blanc S.** 1996. Helper-dependent vector transmission of plant viruses. Annu Rev Phytopathol **34:**227-247.

37. **Schmidt I, Blanc S, Esperandieu P, Kuhl G, Devauchelle G, Louis C, Cerutti M.** 1994. Interaction between the aphid transmission factor and virus particles is a part of the molecular mechanism of cauliflower mosaic virus aphid transmission. Proc Natl Acad Sci U S A **91:**8885-8889.

38. **Blanc S, Lopez-Moya JJ, Wang R, Garcia-Lampasona S, Thornbury DW, Pirone TP.** 1997. A specific interaction between coat protein and helper component correlates with aphid transmission of a potyvirus. Virology **231:**141-147.

633 39. **Blanc S, Ammar ED, Garcia-Lampasona S, Dolja VV, Llave C, Baker J, Pirone TP.** 1998. Mutations
634 in the potyvirus helper component protein: effects on interactions with virions and aphid stylets.
635 J Gen Virol **79 (Pt 12):**3119-3122.
636 40. **Moreno A, Hebrard E, Uzest M, Blanc S, Fereres A.** 2005. A single amino acid position in the
637 helper component of cauliflower mosaic virus can change the spectrum of transmitting vector
638 species. J Virol **79:**13587-13593.
639 41. **Uzest M, Gargani D, Drucker M, Hebrard E, Garzo E, Candresse T, Fereres A, Blanc S.** 2007. A
640 protein key to plant virus transmission at the tip of the insect vector stylet. Proc Natl Acad Sci U S
641 A **104:**17959-17964.
642 42. **Lu G, Li S, Zhou C, Qian X, Xiang Q, Yang T, Wu J, Zhou X, Zhou Y, Ding XS, Tao X.** 2019.
643 Tenuivirus utilizes its glycoprotein as a helper component to overcome insect midgut barriers for
644 its circulative and propagative transmission. PLoS Pathog **15:**e1007655.
645 43. **Ji XL, Yu NT, Qu L, Li BB, Liu ZX.** 2019. Banana bunchy top virus (BBTV) nuclear shuttle protein
646 interacts and re-distributes BBTV coat protein in Nicotiana benthamiana. 3 Biotech **9:**121.
647 44. **Yu N WJ, Yu N, Zheng X, Zhou Q, Liu Z.** 2019. Bioinformatics analysis of the interaction between
648 coat protein and nuclear shuttle protein in babuvirus. Am J plant Sci **10:**622-630.
649 45. **Sicard A, Michalakis Y, Gutierrez S, Blanc S.** 2016. The Strange Lifestyle of Multipartite Viruses.
650 PLoS Pathog **12:**e1005819.
651 46. **Lucia-Sanz A, Manrubia S.** 2017. Multipartite viruses: adaptive trick or evolutionary treat? NPJ
652 Syst Biol Appl **3:**34.
653 47. **Gallet R, Fabre F, Thebaud G, Sofonea MT, Sicard A, Blanc S, Michalakis Y.** 2018. Small
654 Bottleneck Size in a Highly Multipartite Virus during a Complete Infection Cycle. J Virol
655 **92:**e00139-18.
656 48. **Czosnek H, Ghanim M, Ghanim M.** 2002. The circulative pathway of begomoviruses in the
657 whitefly vector Bemisia tabaci - insights from studies with Tomato yellow leaf curl virus. Annals
658 of Applied Biology **140:**215-231.
659 49. **Franz A, Makkouk KM, Vetten HJ.** 1997. Host range of faba bean necrotic yellows virus and
660 potential yield loss in infected faba bean. Phytopathol Medit **36:**94-103.
661 50. **Grigoras I, Timchenko T, Katul L, Grande-Perez A, Vetten HJ, Gronenborn B.** 2009.
662 Reconstitution of authentic nanovirus from multiple cloned DNAs. J Virol **83:**10778-10787.

51. **Sicard A.** 2014. Fonctionnement des populations de virus multipartites de plantes au cours des différentes étapes de leur cycle de vie (Thèse de doctorat).195p. https://prodinra.inra.fr/record/284720.
52. **Akey DH BS.** 1971. Continuous rearing of the pea aphid, Acyrthosophon pisum, on a holidic diet. Ann Entomol Soc Am **64:**353-356.
53. **Vernerey M, Pirolles P, Sicard A.** 2019. Localizing Genome Segments and Protein Products of a Multipartite Virus in Host Plant Cells. Bio Protoc **9(23)**:e3443.
54. **Ghanim M, Brumin M, Popovski S.** 2009. A simple, rapid and inexpensive method for localization of Tomato yellow leaf curl virus and Potato leafroll virus in plant and insect vectors. J Virol Methods **159:**311-314.
55. **Franz A MK, Katul L, Vetten HJ.** 1996. Monoclonal antibodies for the detection and differentiation of Faba bean necrotic yellows virus isolates. Ann Appl Biol**:**255-268.
56. **Lin GW, Chang CC.** 2016. Identification of Critical Conditions for Immunostaining in the Pea Aphid Embryos: Increasing Tissue Permeability and Decreasing Background Staining. J Vis Exp doi:10.3791/53883**:**e53883.
57. **Sicard A, Yvon M, Timchenko T, Gronenborn B, Michalakis Y, Gutierrez S, Blanc S.** 2013. Gene copy number is differentially regulated in a multipartite virus. Nat Commun **4:**2248.
58. **Gallet R, Fabre F, Michalakis Y, Blanc S.** 2017. The number of target molecules of the amplification step limits accuracy and sensitivity in ultra deep sequencing viral population studies. J Virol doi:10.1128/JVI.00561-17.

684

685

686 Figure 1

687

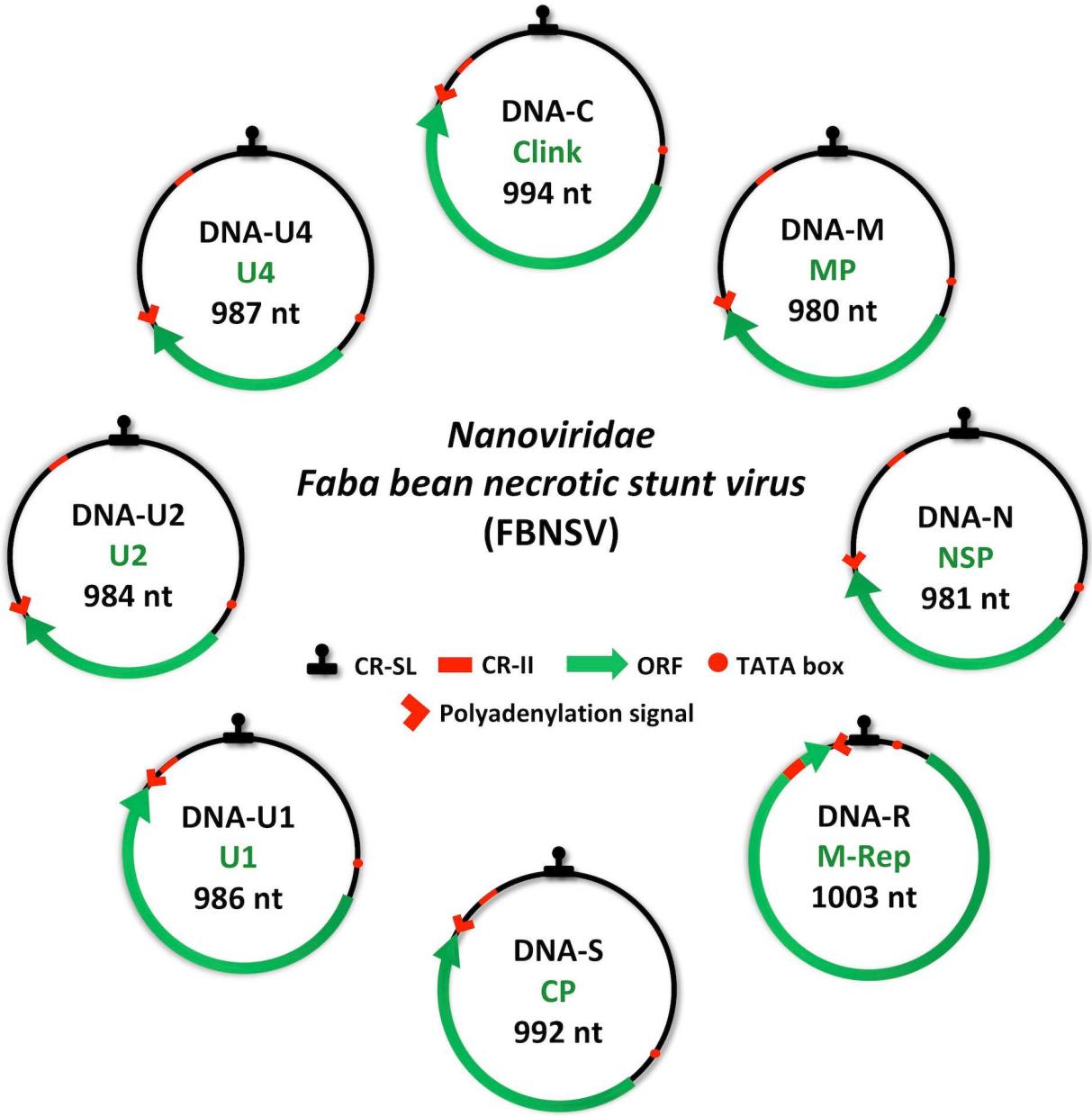

688

689

690 Figure 2

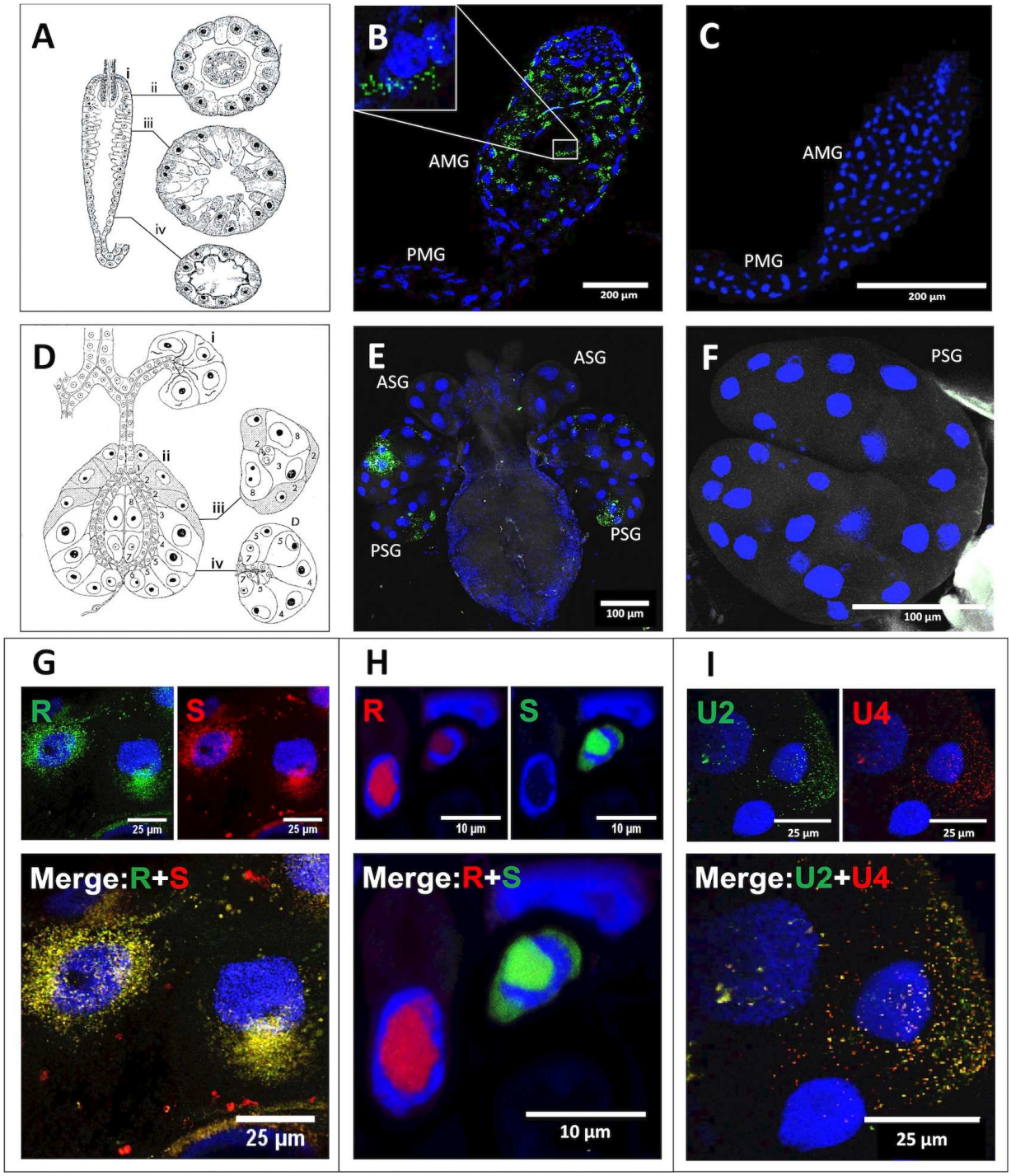

691

692

693 Figure 3

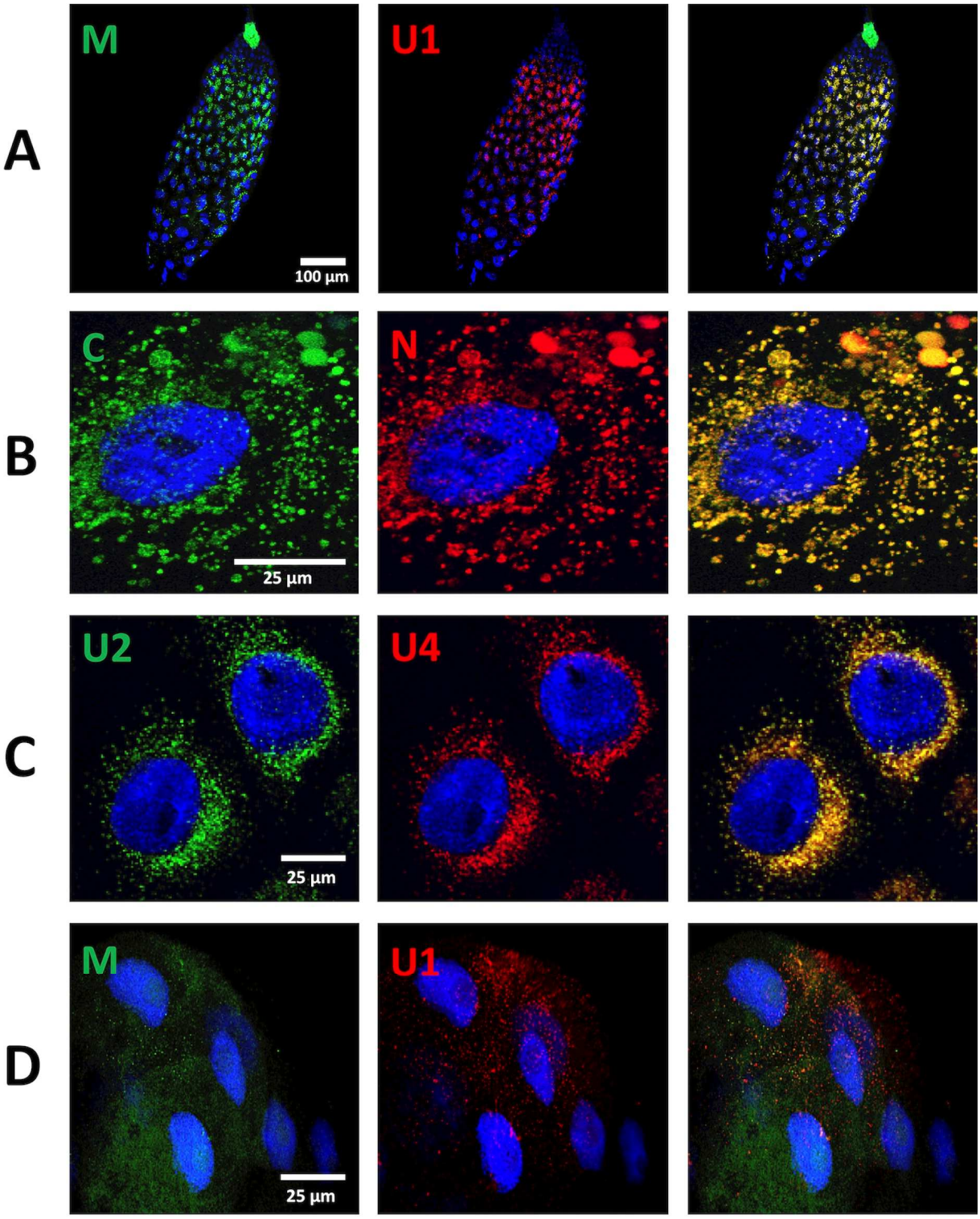

694

695

696 Figure 4

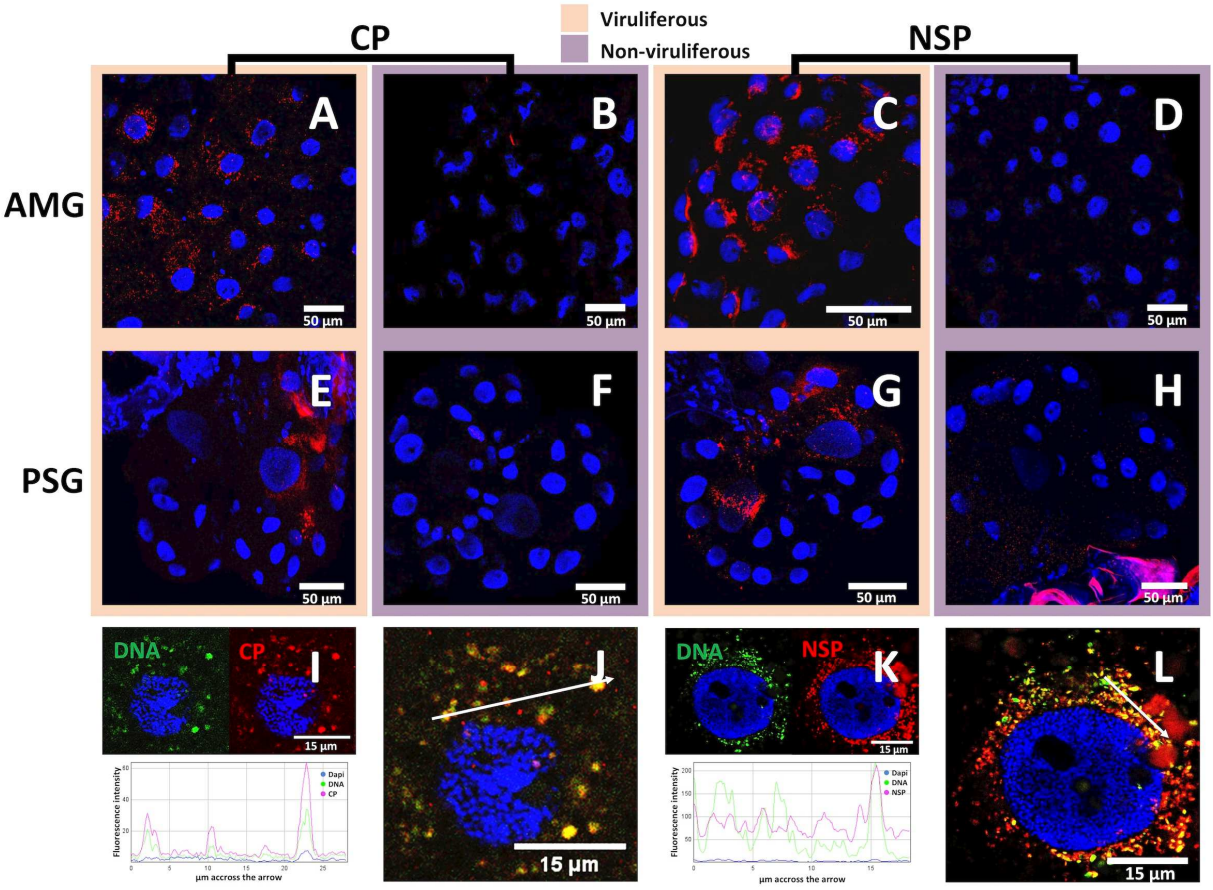

697

698

699 Figure 5

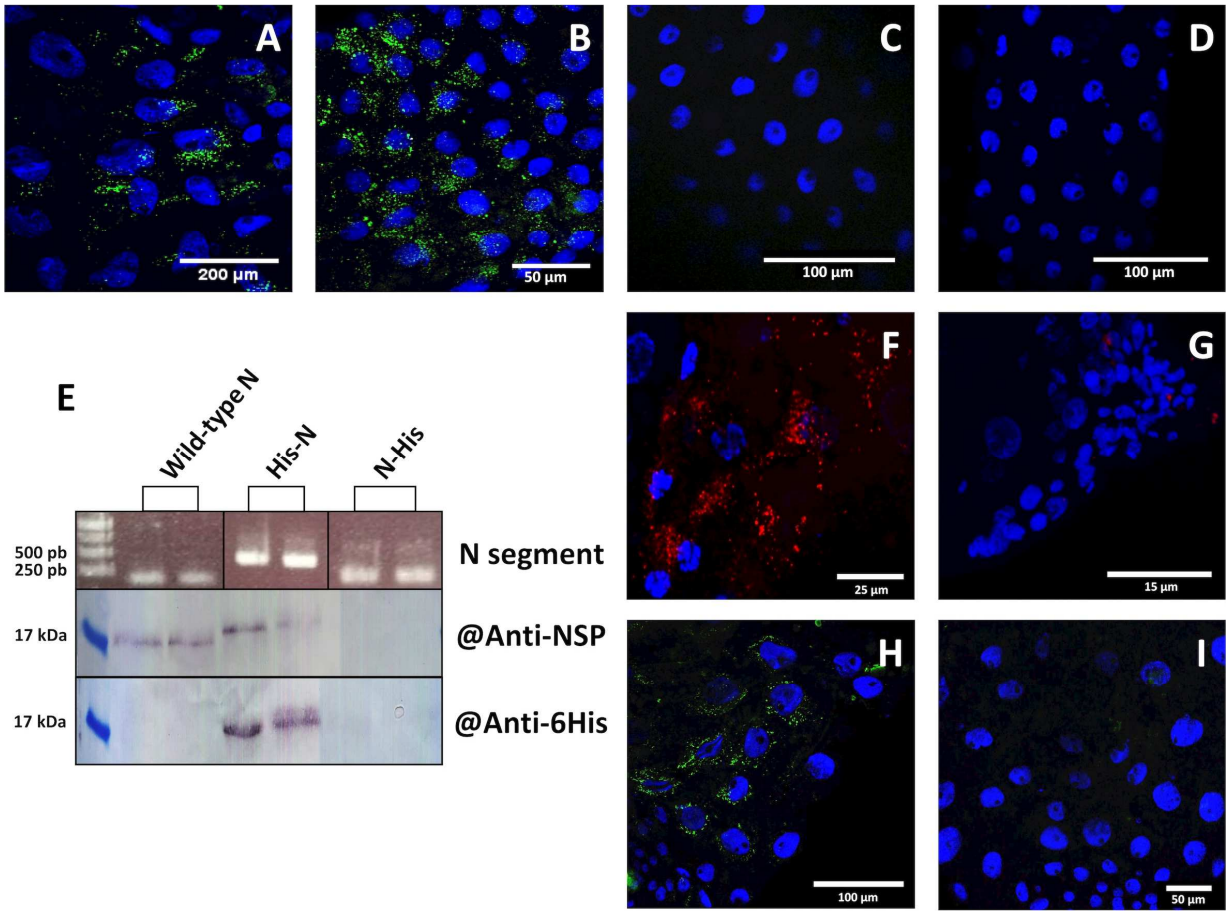

700